

Modeling Carbon Export Out of Mature Peach Leaves¹

Annick Moing^{2*}, Abraham Escobar-Gutiérrez³, and Jean Pierre Gaudillère

Institut National de la Recherche Agronomique, Station de Recherches Fruitières, Centre de Recherches de Bordeaux, BP81 F-33883 Villenave d'Ornon, France (A.M.); and Station de Physiologie Végétale, Centre de Recherches de Bordeaux, BP81 F-33883 Villenave d'Ornon, France (A.E.-G., J.P.G.)

The characteristics of sorbitol and sucrose export out of mature leaves in seedlings of peach (*Prunus persica* L. Batsch cv GF 305) were investigated by simulating carbon fluxes through the leaf. Three treatments were employed: a control treatment and two treatments modifying leaf export, the latter using either shading or girdling. Photosynthesis and ¹⁴C partitioning into sorbitol and sucrose were measured during carbohydrate pool buildup at the beginning of the photoperiod, and the export rate of sorbitol and sucrose was modeled using a PSPICE (Simulation Program with Integrated Circuit Emphasis) simulator. The simulation allowed prediction of the resulting sorbitol and sucrose contents, which were compared to experimental carbohydrate contents. The apparent K_m for sorbitol and sucrose phloem loading, estimated by carbon flux modeling, was 6.6 and 4 mol m⁻³, respectively. The predicted export capacity of the leaf, characterized by the estimated V_{max} values for phloem loading of sorbitol and sucrose, was similar to the photosynthetic carbon flux measured under the leaf growth conditions. This export capacity was enhanced in plants in which all leaves except those studied were shaded. The mature leaf had a higher storage capacity for sorbitol than for sucrose in control plants, especially in the girdled treatment. Sucrose content appears to be tightly regulated.

In most higher plants the primary photosynthetic products are Suc and starch. Both may be stored in the leaf blade during the photoperiod. In addition, sorbitol is reported to be a major photoassimilate in the woody Rosaceae (Wallaart, 1980; Bielecki, 1982), where it is also translocated via phloem (Zimmerman and Ziegler, 1975; Moing et al., 1992). However, information on the regulation of the respective export of sorbitol and Suc is scarce.

Sorbitol biosynthesis involves aldose-6-P reductase (EC 1.1.1.200) (Hirai, 1981; Negm and Loescher, 1981). The catabolic pathways of sorbitol, involving sorbitol dehydrogenases (Negm and Loescher, 1979; Yamaki and Ishikawa, 1986) or sorbitol oxidase (Yamaki, 1980), are not expressed in mature leaves (Loescher et al., 1982; Bielecki and Regdwell, 1985; Merlo and Passera, 1991). Therefore, the fate of sorbitol

in mature leaves is either translocation or storage. The respective role of Suc and sorbitol, both exportable carbohydrates via phloem, in C translocation remains unclear. The pathway and mechanism of phloem loading is still controversial (Van Bel, 1993). Structural studies do not exclude symplastic phloem loading in *Prunus* (Gamalei, 1989), although apoplastic phloem loading would appear more probable, owing to the concentration gradients from mesophyll to phloem for Suc and sorbitol (Moing et al., 1992).

The presence of Suc transporters in the plasma membrane is now well established because their biochemical characteristics have been described in particular by Bush (1989). A plant Suc transporter has been cloned (Riesmeier et al., 1992), and its expression in minor veins indicates a possible role in phloem loading (Riesmeier et al., 1993). However, less information is available concerning alditol transporters. Sorbitol transporters in the tonoplast (Yamaki, 1987) or in protoplasts (Yamaki and Asakura, 1988) have been characterized in apple fruit. However, data concerning the sorbitol transporter from the plasma membrane in green tissues remain unpublished.

A new approach to the mechanistic modeling of C fluxes at the whole-plant level introduces saturable functions (Cheeseman, 1993). Therefore, the apparent kinetic parameters for loading and unloading of assimilates in vivo are required to run these models. For phloem transport, this approach has been illustrated by Minchin et al. (1993) for unloading. In the present work we use a similar approach for phloem loading and we propose a method for estimating the apparent kinetic characteristics (K_m and V_{max}) for loading of sorbitol and Suc in source leaves in vivo. Based on actual measurements of photosynthesis and carbon partitioning into sorbitol and Suc, and simulating the export of these two carbohydrates, we subsequently compared simulated values with actual values of carbohydrate content. C flux modeling was performed using PSPICE (Simulation Program with Integrated Circuit Emphasis) simulator (Nagel, 1975).

MATERIALS AND METHODS

Plant Material

Peach (*Prunus persica* L. Batsch cv GF 305) seedlings were used at the 2-month-old stage. After germination, seedlings

Abbreviations: K_m , apparent Michaelis constant for phloem loading; L , loading rate; L_{max} , maximum phloem loading rate; S , total leaf content of exportable carbohydrate; S_{min} , minimal content of exportable carbohydrate below which no export occurs.

¹ A.E.-G. is the recipient of a fellowship from the Mexican Council for Science and Technology (CONACYT).

² Present address: Institut National de la Recherche Agronomique, Station de Physiologie Végétale, Centre de Recherches de Bordeaux, BP81 F-33883 Villenave d'Ornon, France.

³ Permanent address: Centro Regional de Estudios en Zonas Áridas y Semiaridas-Colegio de Postgraduados, 56230 Chapingo, México.

* Corresponding author; fax 33-56-84-32-45.

were potted and trained to a single shoot. They were cultivated in a growth chamber maintained at 25°C day/20°C night and 80% RH, with a 15-h photoperiod provided by Na-vapor lamps (Phillips SON-T) giving 200 $\mu\text{mol photons m}^{-2} \text{s}^{-1}$ in the 400 to 700 nm range at plant height. The CO_2 concentration was approximately 400 $\mu\text{L L}^{-1}$. For fertilization, Osmocote (15% N, 10% P, 12% K; Sierra Chemical Company, Heerlen, The Netherlands) and Fe-ethylenediamine-*N,N*-di(2-hydroxy-5-methylphenyl)acetic acid (150 mg per pot) were added to the substrate (peat:sand:soil, 1:1:1 by volume) once a month and once a week, respectively.

The second and third youngest mature leaf of a plant were studied during one photoperiod. These two mature leaves were maintained horizontally to avoid a light gradient along the leaf blade the day before the experiment and during the experiment. Their mean surface area was about 35 cm^2 .

Geiger and Fondy (1980) and Minchin and Thorpe (1992) showed that shading of the whole plant, either in the presence or absence of source leaf illumination, increased the sink demand. Conversely, steam girdling of the petiole was shown to decrease phloem loading and affect C partitioning (Ntsika and Delrot, 1986; Goldschmidt and Huber, 1992). To modify the export rate out of the studied leaves, two similar treatments were applied at the start of the experiment on nine plants (four plants for leaf sampling, three plants for photosynthesis measurement, and two plants for ^{14}C partitioning measurement) just before the beginning of the photoperiod. They were compared to nine control plants. In the first treatment all leaves, except the two selected source leaves, were shaded during the day of the experiment. In the second treatment the petiole of the two selected source leaves was rapidly heated with steam after collection of the first sample at the start of the photoperiod. These two treatments were referred to as "shaded plants" and "plants with girdled petioles," respectively. The leaves with steam-girdled petioles remained fully turgid throughout the experiment (data not shown).

Leaf discs (1 cm^2) were removed from the two selected mature leaves on each side of the main vein 0, 1, 2, 4, and 6 h after the start of the photoperiod and at the end of the photoperiod on four plants. The samples were fixed and extracted immediately after collection.

Photosynthesis

Net photosynthetic rate was measured 0, 1, 2, 4, and 6 h after the start of the photoperiod on one young, mature, attached leaf in each of three plants on which no sample was collected, using an IRGA, a dew-point hygrometer, and a mass-flow meter (Gaudillère et al., 1987). Light level and CO_2 concentration were the same as in the growth chamber. Samples were harvested on leaves of exactly similar age from the other plants for biochemical analysis.

Carbon Partitioning

Carbon partitioning into starch was calculated from the derivative of starch content as a function of time, divided by the photosynthetic rate. Carbon partitioning into sorbitol, Suc, and an insoluble residue was determined using $^{14}\text{CO}_2$

pulse labeling on two plants at 0, 1, 2, 4, and 6 h after the beginning of the photoperiod for the control treatment, and at 1, 2, 4, and 6 h after the beginning of the photoperiod for the other two treatments. A portion of an attached leaf was inserted into a 75-mm-long chamber and fed with 3700 MBq $\text{mol}^{-1} \text{ }^{14}\text{CO}_2$ at a concentration of 400 $\mu\text{L L}^{-1}$ for 4 min. After a chase of 2 min with the same concentration of $^{12}\text{CO}_2$ the leaf was removed from the small chamber and two discs (0.5 cm^2 on each side of the main vein in the middle of the leaf blade) were cut rapidly from the leaf. The discs were immediately fixed and extracted in hot ethanol:water (80:20 [v/v] at 80°C) and re-extracted in hot ethanol:water (50:50 [v/v] at 80°C). The soluble fraction was separated into anionic, cationic, and neutral fractions using ion-exchange resins (Dowex 50W in the H^+ form eluted with 1.4 M NH_4OH , and Bio-Rad AG1X8 in the carbonate form eluted with 1 M HCl). Radioactivity in sorbitol and Suc was determined in the soluble neutral fraction using HPLC as described previously (Moing et al., 1992). Residual radioactivity was measured in the pellet after starch hydrolysis (Moing et al., 1992) using tissue solubilizer (NCS, Amersham, UK). Radioactivity in the different fractions was determined using a Packard Tri-Carb 2000 CA liquid scintillation spectrophotometer with Aqualuma Plus (from Lumac-LSC, Groningen, The Netherlands) as scintillant, with external standardization for quenching correction. The sorbitol-to-Suc C partitioning ratio was calculated as the ratio of radioactivity in sorbitol to that in Suc.

Carbohydrate Content

Four plants were sampled for each treatment. The discs collected at the beginning of the photoperiod were cut at the distal side of the two leaf blades, and the discs collected later into the photoperiod were cut closer and closer to the petiole side. In a preliminary experiment (data not shown) we verified that no significant gradient existed along the leaf blade for soluble carbohydrate content expressed on a leaf area basis. Soluble sugars were extracted with hot ethanol:water, purified on tandem ion-exchange resins, and analyzed by HPLC as described previously (Moing et al., 1992). Starch was determined in the pellets after heating at 135°C for 1 h, followed by hydrolysis with amyloglucosidase (EC 3.2.1.3., Merck) and analysis of the Glc levels by HPLC. For comparative purposes, carbohydrate contents were expressed as mol of carbon per unit leaf area.

Flux Modeling

The Model

The model describes the sorbitol and Suc pool buildup at the beginning of the photoperiod. The kinetics of this buildup result from the balance between net photosynthesis and export, since sorbitol is not and Suc is poorly catabolized by the mature leaf. After some hours, biochemical steady state is observed when the synthesis rate of exportable carbohydrates exactly equals their export rate.

For sorbitol and Suc separately, we assumed that the loading rate (L) of the considered carbohydrate could be described by a Michaelis-Menten function:

$$L = L_{\text{max}} \times (S - S_{\text{min}}) / (K_m + [S - S_{\text{min}}])$$

where S is the total leaf content of the considered carbohydrate; S_{min} is the total leaf content of the considered carbohydrate below which the carbohydrate is not exported; L_{max} is the maximum export rate; and K_m is the Michaelis constant. S_{min} was used to take into account the fact that the whole-leaf carbohydrate content was not available for phloem transport as a result of compartmentation.

The simplified model used for simulation is described in Figure 1. It was fed with the measured net photosynthetic rate, the initial content of carbohydrates, and the percent of carbon partitioned into starch and insoluble residue and into total soluble photoassimilates.

Because net photosynthetic rate and C partitioning changed with time during the first half of the photoperiod (Fig. 2, A-C), curve fitting of these parameters as a function of time was realized with Fig.P software (Fig.P Corp., Durham, NC) using a least-square iterative method. For photosynthesis and sorbitol-to-Suc C partitioning ratio, linear and nonlinear regressions were tested until the r coefficient was equal to or greater than 0.8. For C partitioning into starch, a logistic function was used for the control and shaded plants. These equations versus time were introduced in the model (see Appendix).

To solve the model we used a PSPICE (Simulation with Integrated Circuit Emphasis; University of California, Berkeley; Nagel, 1975) software (The Design Center software, version 5.1 from MicroSim Corp., Irvine, CA). PSPICE electrical network simulator has been used for behavioral simulation in biology (Mikulecky, 1983). This simulator, which has been used for water flux modeling (Moltz et al., 1979), is also suitable for C flux modeling. The simulator was fed with the model structure (pool types and pool sizes) and with the transfer functions between the different pools (Fig. 1). The input functions, net photosynthesis, and C partitioning were also introduced, and a time-driven simulation was run. The software gave a numerical and a graphical output that was readily compared with experimental data. Some PSPICE

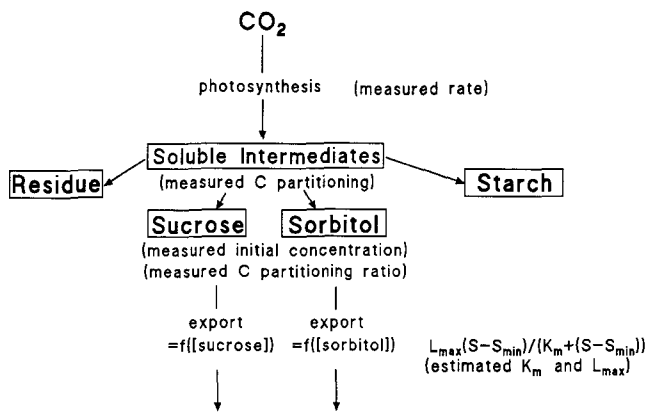


Figure 1. Simplified model for C fluxes in mature peach leaf. Photosynthetic C is partitioned into starch, insoluble residue, and soluble intermediates. Soluble compounds are exported via phloem as either sorbitol or Suc. Measured variables are indicated in parentheses. Export (phloem loading) rate is modeled using a Michaelis-Menten function of carbohydrate content.

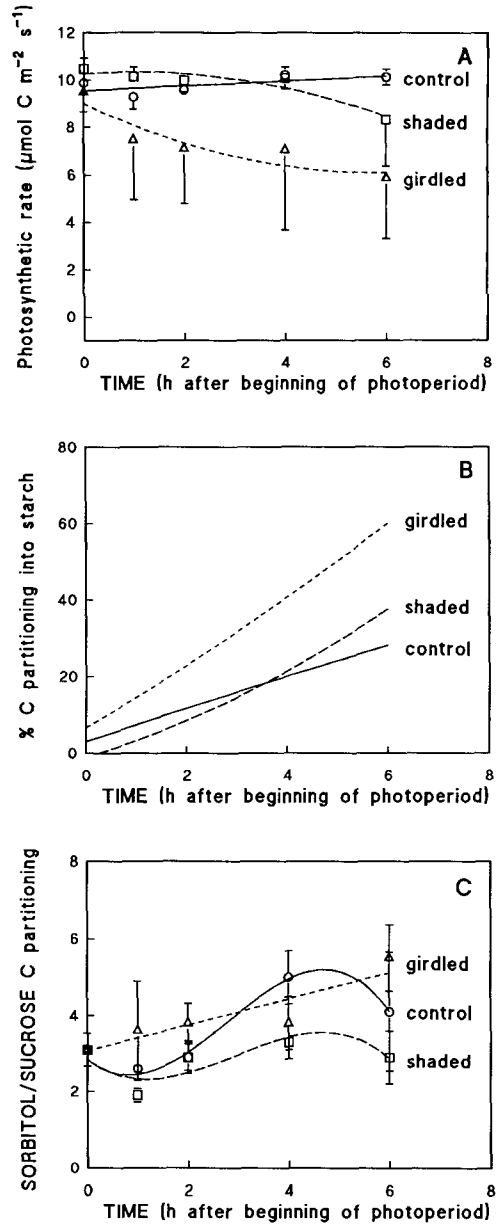


Figure 2. Changes in net photosynthetic rate or C partitioning in mature leaves of control and treated peach seedlings during the first 6 h of the photoperiod. The symbols are the means. Vertical bars represent the standard deviation. The lines represent curve fitting, the equation of which was introduced into the C flux model. A, Changes in photosynthetic rate. The symbols are the mean of three leaves (one leaf per plant, on three plants). B, Changes in C partitioning into starch calculated from the derivative of mean starch content as a function of time divided by photosynthetic rate. C, Changes in sorbitol-to-Suc carbon partitioning ratio calculated using pulse-chase labeling. The symbols are the means of four leaves (two leaves per seedling, on two seedlings).

specifications and the electrical network, analogous to the leaf model and used in the present work, are described in Tables I and II and Figure 6.

The ratio of radioactivity in sorbitol divided by that in Suc is a measure of the sorbitol-to-Suc carbon partitioning ratio, since these two carbohydrates proceed from the same precursor, Glc-6-P (Negm and Loescher, 1981). In a preliminary experiment (data not shown) we verified that, after a pulse labeling, the sorbitol-to-Suc carbon partitioning ratio was constant for a chase of 2 to 30 min. Therefore, we hypothesized that all the carbon not partitioned into starch and insoluble residue will be distributed throughout the sorbitol and Suc pools in the same ratio as the sorbitol-to-Suc carbon partitioning ratio determined 2 min after pulse labeling. In short, the model inputs are based on two coefficients of C partitioning: one between soluble and insoluble photoassimilates and the other between sorbitol and Suc.

Contents were expressed as mol carbon per unit leaf area in order to facilitate comparison with net photosynthetic rate values, the latter usually expressed as flux densities. However, when leaf compartmentation is not taken into account, global concentrations can be easily calculated, given that the mean leaf dry weight per unit area was $26.8 \pm 2.8 \text{ g m}^{-2}$ ($n = 144$), with a water content of about 63 mL m^{-2} .

Using the simulator to calculate sorbitol and Suc leaf contents, we estimated K_m , L_{max} , and S_{min} for both sorbitol and Suc. The PSPICE programs used for calculation are described in the Appendix.

Model Parameters

The photosynthesis and carbon partitioning parameters used originated from the present experimental data. For both exportable carbohydrates the values for S_{min} were determined by fitting the initial part of the calculated content to the measured content. Apparent K_m values were tested from 6 mol C m^{-3} (i.e. $380 \mu\text{mol C m}^{-2}$) to 60 mol C m^{-3} (i.e. $3800 \mu\text{mol C m}^{-2}$) according to the kinetic characteristics of Suc transporters in the plasma membrane reported by Delrot (1989), Bush (1993), and Riesmeier et al. (1992). L_{max} values were tested between 1 and 100 times the measured carbon flux in each carbohydrate. For a given K_m , L_{max} was randomly tested to fit the calculated carbohydrate content to the measured carbohydrate content.

Implicit Hypotheses

Two basic hypotheses sustain the model. First, the fact that all soluble photoassimilates are potentially exportable and

that sorbitol and Suc are not significantly metabolized in the mature leaf in the light. Second, for phloem loading we assumed that, in the physiological range of carbohydrate concentrations, only one transporter was functioning for each exportable carbohydrate, with constant kinetic parameters throughout the experiment.

RESULTS

Photosynthetic Rate

Net photosynthetic rate remained constant during the first half of the photoperiod in control plants (Fig. 2A). Its mean value was $9.8 \pm 0.5 \mu\text{mol C m}^{-2} \text{ s}^{-1}$ ($n = 15$). It decreased with time and was very variable within treatments compared to the control (Fig. 2A). The photosynthetic rate of shaded plants did not differ significantly from that of control plants from 0 to 4 h after the beginning of the photoperiod. However, it decreased 6 h after the beginning of the photoperiod. For plants with girdled petioles, photosynthetic rate decreased about 20% soon after the treatment and then remained constant.

Measured Changes in Partitioning of Photosynthetic C in Source Leaves during the Photoperiod

Partitioning of photosynthetic carbon changed with time during the first 6 h of the photoperiod. It was also affected by the treatment. The percent carbon partitioned into starch increased from 0 to 6 h after the beginning of the photoperiod for all treatments (Fig. 2B). Partitioning into starch in the control was not different from partitioning in the shaded treatment. Partitioning into starch in plants with girdled petioles was significantly higher than in the two other treatments. It reached a value of about 60% 6 h after the beginning of the photoperiod.

The percent C partitioned into insoluble residue was affected neither by the time nor by the treatment (data not shown). Its mean value \pm SD for all times and treatments was $1\% \pm 1\%$ ($n = 50$).

The sorbitol-to-Suc carbon partitioning ratio (Fig. 2C) increased with time from 0 to 4 h after the beginning of the photoperiod for all treatments, and from 0 to 6 h for the plants with girdled petioles, although statistically significant differences were not always observed. It decreased from 4 to 6 h after the beginning of the photoperiod for the control and shaded treatments.

The percent C partitioned into starch and the sorbitol-to-Suc carbon partitioning ratio used for the carbon flux model

Table I. Units and parameters for PSPICE programs simulating C fluxes in mature peach leaf

LEAF Biological Model		SPICE Electrical Device	
Significance	Unit	Device	Code
Carbohydrate pool	m^{-2}	Capacitor	C
Carbohydrate content	mol C m^{-2}	Voltage source	V
Carbon flux density	$\text{mol C m}^{-2} \text{ s}^{-1}$	Current source	g
Simulation utilities to			
Generate utility function	mol C m^{-2}	Voltage source	E
Enforce Kirchoff's law	s	High resistance	R

Table II. Parameters and devices in the electrical system (see Figure 6) analogous to the leaf model

Name	Significance
CInt	Soluble intermediate pool
CRes	Insoluble residue pool
CSor	Sorbitol pool
CStarch	Starch pool
CSuc	Sucrose pool
ELSuc	Device setting gLSuc to zero when V(4) < SminSuc
ELSor	Device setting gLSor to zero when V(5) < SminSor
ESol	Generator for partitioning of photosynthetic C into soluble compounds
ESorSuc	Generator for sorbitol to Suc C partitioning ratio
gLSor	Phloem loading rate for sorbitol
gLSuc	Phloem loading rate for Suc
gPS	Net photosynthetic rate
gRes	Photosynthetic carbon flux into insoluble residue
gSor	Photosynthetic carbon flux into sorbitol pool
gStarch	Photosynthetic carbon flux into starch
gSuc	Photosynthetic carbon flux into Suc pool
KSor	K_m for sorbitol phloem loading
KSuc	K_m for suc phloem loading
LmaxSor	Maximum phloem loading rate for sorbitol
LmaxSuc	Maximum phloem loading rate for Suc
pRes	% C partitioning into insoluble residue
pStarch	% C partitioning into starch
R devices	All devices beginning with R are high resistances used as simulation utilities necessary to run PSPICE but with no effect on the C flux
SminSuc	Leaf Suc content below which no Suc loading occurs
SminSor	Leaf sorbitol content below which no sorbitol loading occurs
VPS	Atmospheric CO ₂ pool in arbitrary units
Vg devices	All devices beginning with Vg are current meters used to measure C flux
Vt	Voltage source generating time in s
V(3)	Leaf residue content
V(4)	Leaf Suc content
V(5)	Leaf sorbitol content
V(6)	Leaf starch content
V(70)	Time
V(80)	% C partitioning into soluble compounds
V(81)	Sorbitol/Suc C partitioning ratio

are represented by the fitted curves on Figure 2, B and C. The equations of these fitted curves are included in Appendix 1. For the residue, the mean value of all times and treatments (1%) was used. C partitioning into soluble photoassimilates was calculated as the difference between total photosynthetic carbon and partitioning into insoluble compounds, i.e. starch plus residue.

Measured Changes in Leaf Carbohydrate Content during the Photoperiod

At the beginning of the photoperiod, the major nonstructural carbohydrates in mature leaves were sorbitol followed by Suc and starch (Fig. 3). Six hours after the beginning of the photoperiod the two major, nonstructural carbohydrates were sorbitol and starch, followed by Suc.

Suc content on a leaf area basis (Fig. 3A) behaved similarly

in both treated and control plants. It increased from about 20 to 30 mmol C m⁻² during the first 2 h of light and then remained stable. Hexose + inositol content (data not shown) increased slightly during the first 4 h of the photoperiod. However, their content at the end of the photoperiod did not differ from that at the beginning of the photoperiod.

Sorbitol was the only soluble carbohydrate for which the content was affected by the applied treatments (Fig. 3B). In control plants during the first part of the photoperiod, sorbitol content increased from 35 to 64 mmol C m⁻². In leaves with girdled petioles this accumulation was even higher, reaching 87 mmol C m⁻² 6 h after the beginning of the photoperiod. In shaded plants sorbitol accumulation was reduced in the normally illuminated leaves.

Starch content expressed on a leaf area basis (Fig. 3C) increased linearly during the photoperiod after a lag period of a few hours. During the first half of the photoperiod, no

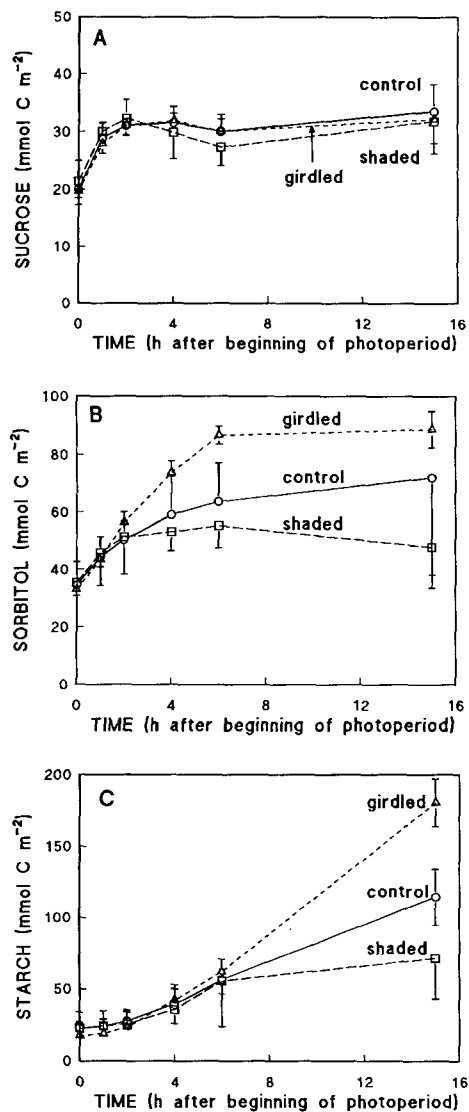


Figure 3. Changes in soluble carbohydrate content in mature leaves of control and treated peach seedlings during a photoperiod. Mean of eight leaves (two leaves per seedling, on four seedlings). Vertical bars represent *sd* values. A, Suc content. B, Sorbitol content. C, Starch content.

significant difference appeared between treated and control plants. However, at the end of the photoperiod leaves with girdled petioles accumulated significantly more starch, and leaves from shaded plants accumulated significantly less starch, than those of control plants.

Simulation of C Export

Due to its calculation mode, the calculated starch content (data not shown) was in good agreement with the measured starch content. The changes in sorbitol and Suc content calculated using the simulation programs described in Appendix 1 are represented by the curves in Figure 4, A to C, for both control and treated plants. The calculated content

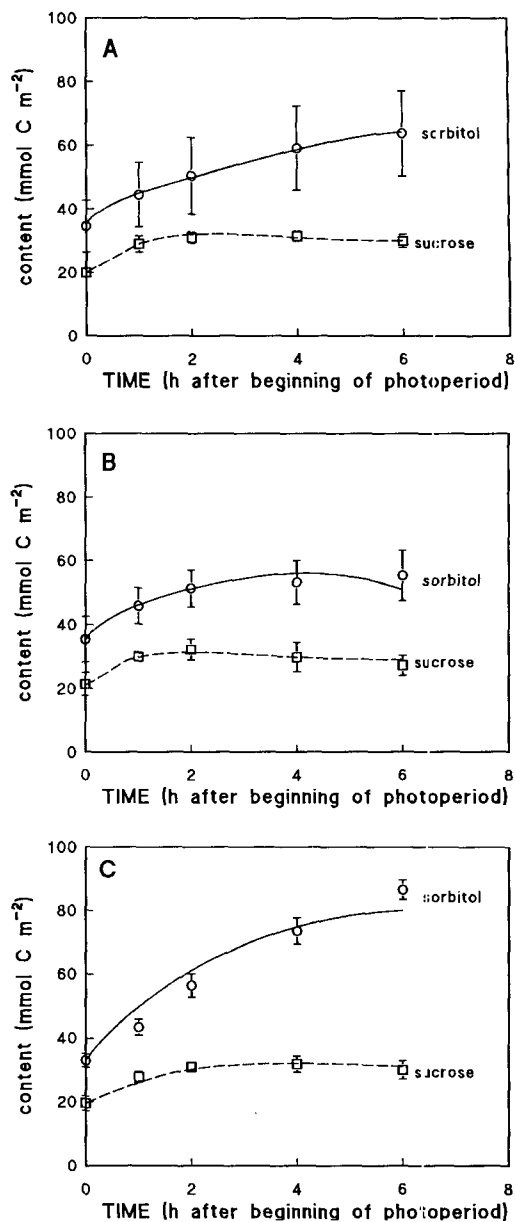


Figure 4. Measured and calculated sorbitol and Suc contents in control plants (A), in shaded plants (B), and in plants with girdled petioles (C). The symbols represent the mean measured contents, the vertical bars represent *sd* values. The curves result from simulation of carbon fluxes with the following parameters for phloem loading. K_m and S_{min} are the same for the control and the two other treatments. L_{max} depends on the treatment. For sorbitol, $K_m = 6.6 \text{ mol m}^{-3}$, $S_{min} = 36 \text{ mmol C m}^{-2}$; $L_{max} = 6.04 \text{ } \mu\text{mol C m}^{-2} \text{ s}^{-1}$ for the control; $L_{max} = 6.4 \text{ } \mu\text{mol C m}^{-2} \text{ s}^{-1}$ for the shaded plants; $L_{max} = 1.9 \text{ } \mu\text{mol C m}^{-2} \text{ s}^{-1}$ for the plants with girdled petioles. For Suc, $K_m = 4.0 \text{ mol m}^{-3}$, $S_{min} = 28 \text{ mmol C m}^{-2}$; $L_{max} = 3.2 \text{ } \mu\text{mol C m}^{-2} \text{ s}^{-1}$ for the control; $L_{max} = 5.0 \text{ } \mu\text{mol C m}^{-2} \text{ s}^{-1}$ for the shaded plants; $L_{max} = 1.2 \text{ } \mu\text{mol C m}^{-2} \text{ s}^{-1}$ for the plants with girdled petioles.

was in good agreement with the measured content for both treatments.

To obtain this good agreement, the selected K_m values were 4 mol m^{-3} for Suc and 6.6 mol m^{-3} for sorbitol. The selected S_{min} values were 28 mmol C m^{-2} for Suc and 36 mmol C m^{-2} for sorbitol. The model inputs included different L_{max} values according to the treatment. For Suc phloem loading, L_{max} values were $3.2, 5.0,$ and $1.2 \text{ } \mu\text{mol C m}^{-2} \text{ s}^{-1}$ for the control, shaded plants, and plants with girdled petioles, respectively. For sorbitol phloem loading, L_{max} values were $6.0, 6.4,$ and $1.9 \text{ } \mu\text{mol C m}^{-2} \text{ s}^{-1}$ for the control, shaded plants, and plants with girdled petioles, respectively.

These three parameters describe the export rates as a function of exportable carbohydrate leaf content presented in Figure 5A for sorbitol and in Figure 5B for Suc. After 2 h of illumination, sorbitol export rate was already very close to its maximum value, and it remained at this maximum value for the rest of the photoperiod in control and treated plants. In contrast, Suc export rate was nil during the first hour after illumination and stayed far below its maximum value during the rest of the photoperiod in control and shaded plants. The shaded treatment increased export rate of sorbitol and Suc, with a higher effect on Suc export. The girdled treatment greatly reduced export rate of sorbitol and Suc.

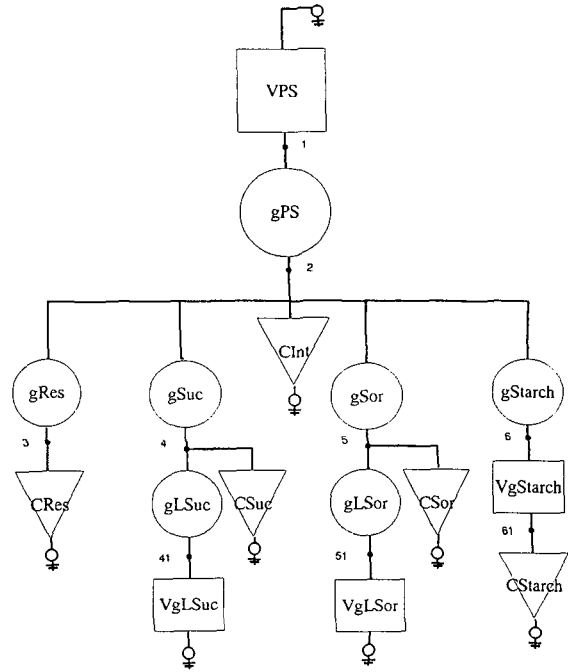


Figure 6. The PSPICE electrical system analogous to the leaf model (see Table II for devices).

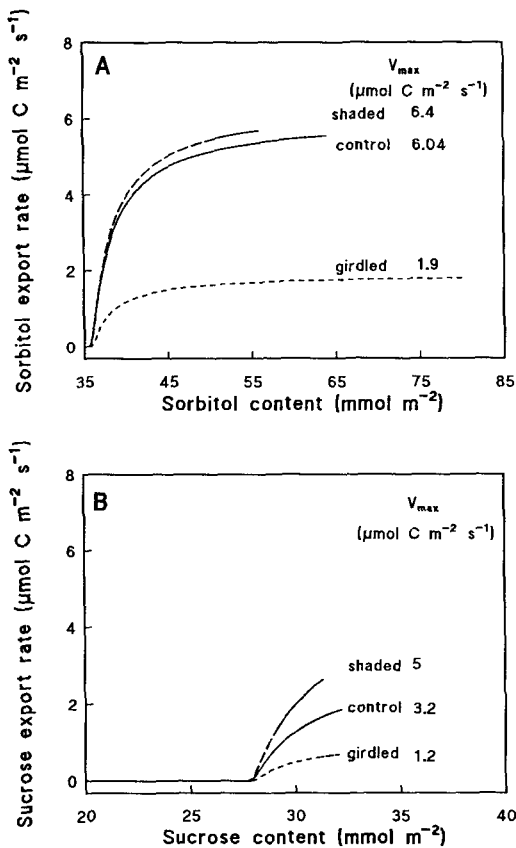


Figure 5. Export rate for control plants, shaded plants, and plants with girdled petioles, calculated with the parameters of the phloem loading model used in Figure 4, A to C, as a function of the total leaf content of each exportable carbohydrate. A, Sorbitol. B, Suc.

DISCUSSION

Modeling carbon fluxes in a mature peach leaf (Fig. 1) allowed us to calculate the apparent kinetic characteristics of sorbitol phloem loading. K_m was calculated for control plants and was assumed to remain constant for shaded and girdled plants. V_{max} was recalculated for these two treatments. The apparent K_m values were calculated from the model as mol of carbon per unit leaf area, and they were expressed as mol m^{-3} , assuming that carbohydrate concentrations were similar in all compartments. The calculated apparent K_m value (6.6 mol m^{-3}) for sorbitol export from the present model is close to the K_m values computed by Yamaki (1987) for sorbitol uptake into isolated fruit vacuoles (5 mol m^{-3}) and by Yamaki and Asakura (1988) for sorbitol import into fruit protoplasts (3.6 mol m^{-3}). The calculated apparent K_m value (4 mol m^{-3}) for Suc phloem loading from the present model is higher than the K_m value reported by Bush (1993) for plasma membrane (1 mol m^{-3}).

The biochemical characterization of an alditol transporter from plasma membrane would help to clarify the present results. Information on mannitol uptake in tissues or isolated organs (Daie, 1986; Keller, 1991) exists, although transporters in plasma membrane vesicles have not yet been characterized.

To fit simulated carbohydrate content with that of the experimental data, C flux modeling predicts an apparent content threshold for carbohydrate export. This threshold, S_{min} (Fig. 5), below which the carbohydrate is not exported, is higher for Suc than for sorbitol. Its physiological basis is tissue or subcellular carbohydrate compartmentation, which was not directly measured in the present study. The vacuole

would be a good candidate for such a transitory storage compartment in mesophyll cells. An active transport of Suc across the tonoplast into the vacuole against a concentration gradient must be hypothesized to explain the delay in Suc export after the beginning of photoperiod. Tonoplast Suc transporters with a K_m value of about 10 mol m^{-3} have been reported (Bush, 1993). However, this hypothesis is not in accordance with the results of Riens et al. (1991) and Winter et al. (1993), who have shown in spinach and barley a lower Suc concentration in vacuole than in cytosol. However, Martinoia (1992) suggested an equilibrium for Suc concentration between vacuole and cytoplasm, with a Suc uptake into the vacuole by facilitated diffusion in photosynthesizing tissues. Vacuolar Suc accumulation, which occurs in typical storage tissues (Martinoia 1992), may therefore be species dependent in photosynthesizing tissues. The fate of sorbitol differs from that of Suc, since sorbitol is concurrently translocated out of the mesophyll and stored in the mesophyll from the beginning of the photoperiod. Therefore, two hypotheses may be proposed. First, in peach, the tonoplast in the source leaf cannot transport sorbitol, contrary to apple fruit tonoplast (Yamaki, 1987), and/or second, vacuolar and cytosolic sorbitol pools are rapidly interchanged in the absence of a concentration gradient for sorbitol between the vacuole and the cytosol.

In control plants and in plants with girdled petioles the mature peach leaf stores 2 times and 5 times more sorbitol than Suc, respectively (Fig. 4, A and C). The content of Suc seems highly regulated. Plant species may be characterized as typical starch storers (soybean; Goldschmidt and Huber, 1992), Suc storers (spinach; Goldschmidt and Huber, 1992), and starch and sorbitol storers (peach). However, in the present experiment sorbitol content reached a plateau 6 h after the beginning of the photoperiod in the leaves with girdled petioles. At this plateau value, sorbitol develops a global osmotic potential of about 0.6 MPa in fully turgescient photosynthesizing leaf blades. Sorbitol storage possibly provides a high capacity for osmoregulation in peach leaves. Osmoregulation by sorbitol has been reported previously for leaves of water-stressed cherry (*Prunus*) trees (Ranney et al., 1991).

The simulation gives an estimate of V_{\max} for the Suc and sorbitol transporters involved in phloem loading (Fig. 5). These estimates are nearly equal to the value of the entering carbon flux (Fig. 2A). A transitory increase in the sink demand, by shading all leaves except the two source leaves, induces a V_{\max} increase for the Suc transporter but not for the sorbitol transporter (Fig. 5). Simulation showed that leaves with girdled petioles continue to export carbohydrates from the leaf mesophyll, although at a much lower V_{\max} than leaves in control plants. We verified (data not shown) that it was not transitory storage in the main vein. Steam girdling may have left a few intact sieve tubes, enabling a reduced phloem sap flow.

The kinetic characteristics of Suc and sorbitol phloem loading estimated using the present simulation cannot be accounted for by a single transporter in phloem plasmalemma. Due to the model structure, these characteristics describe carbohydrate transport from mesophyll to apoplast. Moreover, the effect of sink demand on the apparent V_{\max}

estimated with the present model, indicates that this V_{\max} may also depend on phloem mass flow. The process of carbohydrate efflux out of the mesophyll and diffusion within the apoplast has not been taken into account in the present C flux model from mesophyll to phloem. Suc transport from mesophyll cytoplasm to apoplast may be passive or carrier mediated (Laloi et al., 1993). Owing to the steep gradient for Suc across the mesophyll plasma membrane (Tetlow and Farrar, 1993; Winter et al., 1993), a Suc carrier appears to be inefficient. In fact, the Suc gradient across plasmalemma is in accordance with a simple diffusion through a lipoprotein membrane model (Nobel, 1983).

A simplified model of phloem loading (Figs. 1 and 6), which does not take into account the leaf compartments, predicts the changes in the level of carbohydrates exportable from leaves. Similar measurements and modeling may be used to quantify the effects of apoplastic exogenous chloromercuri-benzenesulfonic acid on sorbitol and Suc fluxes, respectively. The present model, restricted to the source leaf, will be complemented in the future with a model of phloem transport from source to sink to take into account the effect of mass flow on Suc and sorbitol maximum loading rates.

In conclusion, sorbitol and Suc do not follow the same fate in peach leaves. Sorbitol is typically a storage carbohydrate, as is starch. The kinetic pattern of phloem loading, estimated by simulation, results from the functioning of carbohydrate transport from mesophyll into phloem sap. It shows that loading capacities are saturated for sorbitol but not for Suc. The next step would be a more precise description of C flux, including transport through mesophyll plasmalemma and mass flow in phloem sap (Minchin et al., 1993).

APPENDIX

PSPICE Program for Simulating Phloem Loading in Mature Leaves: (Time Units Are Seconds.)

*constant parameters

.param LmaxSuc=1.2e-6, LmaxSor=1.9e-6,
KSuc=3040e-6, KSor=2500e-6, Sminsuc=.28e-3,
Sminsor=.36e-3, pRes=0.01

*photosynthesis

VPS 1 0 1

gPS 1 2 value {1e-6(2.977e-5*V(70)+9.53)}; Control plants

gPS 1 2 value {1e-6(-5.74e-9*pwr(V(70),2)+4.17e-5*V(70)+10.25)}; shaded plants

gPS 1 2 value {1e-6*(6.58e-9*pwr(V(70),2)-2.76e-4*V(70)+8.998)}; plants with girdled petioles

CInt 2 0 1 ic=.5e-3; 500 $\mu\text{mol C m}^{-2}$; intermediary products

*in

gSuc 2 4 value {(V(80)/(1+V(81)))*i(VPS)*(-1)}

*CSuc 4 0 1 ic=20e-3; 20 mmol C m^{-2} Control plants

*CSuc 4 0 1 ic=21e-3; 21 mmol C m^{-2} ; shaded plants

CSuc 4 0 1 ic=19.6e-3; 19.6 mmol C m^{-2} plants with girdled petioles

gSor 2 5 value {(V(81)*V(80)/(1+V(81)))*i(VPS)*(-1)}

*CSor 5 0 1 ic=35e-3; 35 mmol C m^{-2} Control plants

*CSor 5 0 1 ic=35e-3; 35 mmol C m^{-2} ; shaded plants

CSor 5 0 1 ic=33e-3; 33 mmol C m⁻² plants with girdled petioles
 gStarch 2 6 value{-1e-2(11.59e-4*V(70)+3.335)*i(VPS)};
 Control plants
 *gStarch 2 6 value
 {-1e-2*(3.876e-8*pwr(V(70),2)+9.186e-4*V(70)*i(VPS))}; shaded plants
 gStarch 2 6 value
 {-1e-2*(1.534e-8*pwr(V(70),2)+2.143e-3*V(70)+6.694)*i(VPS)}; plants with girdled petioles
 *CStarch 61 0 1 ic=23e-3; 23 mmol C m⁻² Control plants
 *CStarch 61 0 1 ic=23e-3; 23 mmol C m⁻²; shaded plants
 CStarch 61 0 1 ic=17.5e-3; 17.5 mmol C m⁻² plants with girdled petioles
 VgStarch 6 61 0;
 gRes 2 3 value {pRes*i(VPS)*(-1)}
 CRes 3 0 1 ic=0
 *out
 ELSuc 411 0 value {(0+V(4)-Sminsuc+ABS(0-(V(4)-Sminsuc)))/2}; to avoid negative values of V(4)
 gLSuc 4 41 value {(LmaxSuc*V(411))/(V(411)+KSuc)}
 VgLSuc 41 0 0
 ELSor 511 0 value {(0+V(5)-Sminsor+ABS(0-(V(5)-Sminsor)))/2}; to avoid negative values of V(5)
 gLSor 5 51 value {(LmaxSor*V(511))/(V(511)+KSor)}
 VgLSor 51 0 0
 *partitioning utilities
 *ESorSuc 81 0 value
 {((-2e-12)*V(70)*V(70)*V(70))+5.98e-8*V(70)*V(70)-3e-4*V(70)+2.85}; Control plants
 *ESorSuc 81 0 value {(-1.25e-12*V(70)*V(70)*V(70))+3.96e-8*V(70)*V(70)-2.7e-4*V(70)+2.85};
 shaded plants
 ESorSuc 81 0 value {9.483e-5*V(70)+3.072}; plants with girdled petioles
 ESol 80 0 value {1-pRes+(i(VgStarch)/i(VPS))};
 *simulation utilities
 R2 2 0 1e12
 R3 3 0 1e12
 R4 4 0 1e12
 R5 5 0 1e12
 R61 61 0 1e12
 R80 80 0 1e12
 R81 81 0 1e12
 R411 411 0 1e12
 R511 511 0 1e12
 Vt 70 0 pwl (0 0 21600 21600)
 Rt 70 0 1e12
 *commands for numerical and graphical output
 .op
 .tran 100 21600 uic
 .probe
 .print tran V(4) V(5) V(6) i(vgLSor) i(vgLSuc)
 .end

ACKNOWLEDGMENTS

We thank M. Gaudillère for her help with the HPLC analysis and radioactivity measurements of carbohydrates. We acknowledge Dr. P. Raymond and Dr. S. Delrot for critical reading of the manuscript.

Received March 28, 1994; accepted June 27, 1994.
 Copyright Clearance Center: 0032-0889/94/106/0591/10.

LITERATURE CITED

- Bielecki RL** (1982) Sugar alcohols. In FA Loewus, W Tanner, eds, Plant Carbohydrates I. Intracellular Carbohydrates. Encyclopedia of Plant Physiology, New Series, Vol 13A. Springer-Verlag, Berlin, pp 158-192
- Bielecki RL, Regdwell RJ** (1985) Sorbitol versus sucrose as photosynthesis and translocation products in developing apricot leaves. Aust J Plant Physiol 132: 657-668
- Bush DR** (1989) Proton-coupled sucrose transport in plasmalemma vesicles isolated from sugar beet (*Beta vulgaris* L. cv Great Western) leaves. Plant Physiol 89: 1318-1323
- Bush DR** (1993) Proton-coupled sugar and amino acid transporters in plants. Annu Rev Plant Physiol Plant Mol Biol 44: 513-542
- Cheeseman JM** (1993) Plant growth modelling without integrating mechanisms. Plant Cell Environ 16: 137-147
- Daie J** (1986) Kinetics of sugar transport in isolated vascular bundles and phloem tissue of celery. J Am Soc Hortic Sci 111: 216-220
- Delrot S** (1989) Loading of photoassimilates. In DA Baker, JA Milburn, eds, Transport of Photoassimilates. Longman Scientific & Technical, London, pp 167-205
- Gamalei Y** (1989) Structure and function of leaf minor veins in trees and herbs. A taxonomic review. Trees 3: 96-110
- Gaudillère JP, Bernoud JJ, Jardinot JP, Euvrard M** (1987) Effect of periodic fluctuations of photon flux density on photosynthetic characteristics of soybean leaves. Photosynth Res 13: 81-89
- Geiger DR, Fondy BR** (1980) Response of phloem loading and export to rapid changes in sink demand. In W Eschrich, H Lorenzen, eds, Phloem Loading and Related Processes. Gustav Fisher Verlag, Stuttgart, Germany, pp 177-186
- Goldschmidt EE, Huber SC** (1992) Regulation of photosynthesis by end-product accumulation in leaves of plants storing starch, sucrose, and hexose sugars. Plant Physiol 99: 1443-1448
- Hirai M** (1981) Purification and characteristics of sorbitol-6-phosphate dehydrogenase from loquat leaves. Plant Physiol 67: 221-224
- Keller F** (1991) Carbohydrate transport in discs of storage parenchyma of celery petioles. 2. Uptake of mannitol. New Phytol 117: 423-429
- Laloi M, Delrot S, M'Batchi B** (1993) Characterization of sugar efflux from sugar beet leaf plasma membrane vesicles. Plant Physiol Biochem 31: 731-741
- Loescher WH, Marlow GC, Kennedy RA** (1982) Sorbitol metabolism and sink-source interconversions in developing apple leaves. Plant Physiol 70: 335-339
- Martinoia E** (1992) Transport processes in vacuoles of higher plants. Bot Acta 105: 232-245
- Merlo L, Passera C** (1991) Changes in carbohydrate and enzyme levels during development of leaves of *Prunus persica*, a sorbitol synthesizing species. Physiol Plant 83: 621-626
- Mikulecky DC** (1983) Network thermodynamics: a candidate for a common language for theoretical and experimental biology. Am J Physiol 245: (Regulatory Integrative Comp Physiol 14) R1-R9
- Minchin PEH, Thorpe MR** (1992) Carbon 11 in the study of phloem translocation. In CJ Pollack, JF Farrar, AJ Gordon, eds, Carbon Partitioning Within and Between Organisms. Bios Scientific Publishers, Oxford UK, pp 225-247
- Minchin PEH, Thorpe MR, Farrar JF** (1993) A simple mechanistic model of phloem transport which explains sink priority. J Exp Bot 44: 947-955
- Moing A, Carbonne F, Rashad MH, Gaudillère JP** (1992) Carbon fluxes in mature peach leaves. Plant Physiol 100: 1878-1884
- Moltz FJ, Kerns DV Jr, Peterson CM, Dane IM** (1979) A circuit analog model for studying quantitative water relations of plant tissues. Plant Physiol 64: 712-716
- Nagel L** (1975) SPICE 2. A Computer Program to Simulate Semiconductor Circuits. Memorandum ERL-M 520. Electronics Research Laboratory, College of Engineering, University of California, Berkeley

- Negm FB, Loescher WH** (1979) Detection and characterization of sorbitol dehydrogenase from apple callus tissue. *Plant Physiol* **64**: 69–73
- Negm FB, Loescher WH** (1981) Characterization and partial purification of aldose-6-phosphate reductase (alditol-6-phosphate: NADP 1-oxidoreductase) from apple leaves. *Plant Physiol* **67**: 139–142
- Nobel PS** (1983) Cell and diffusion. In *Biophysical Plant Physiology and Ecology*. WH Freeman and Co, New York, pp 1–47
- Ntsika G, Delrot S** (1986) Changes in apoplastic and intracellular leaf sugars induced by the blocking of export in *Vicia faba*. *Physiol Plant* **68**: 145–153
- Ranney TG, Bassuk NL, Whitlow TH** (1991) Osmotic adjustment and solute constituents in leaves and roots of water-stressed cherry (*Prunus*) trees. *J Am Soc Hortic Sci* **116**: 684–688
- Riens B, Lohaus G, Heineke D, Heldt HW** (1991) Amino-acid and sucrose content determined in the cytosolic, chloroplastic and vacuolar compartment and in the phloem sap of spinach leaves. *Plant Physiol* **97**: 227–233
- Riesmeier W, Hirner B, Frommer WB** (1993) Potato sucrose transporter expression in minor veins indicates a role in phloem loading. *Plant Cell* **5**: 1591–1598
- Riesmeier W, Willmitzer L, Frommer WB** (1992) Isolation and characterization of a sucrose carrier cDNA from spinach by functional expression in yeast. *EMBO J* **11**: 4705–4713
- Tetlow IJ, Farrar JF** (1993) Apoplastic sugar concentration and pH in barley leaves infected with brown rust. *J Exp Bot* **44**: 929–936
- Van Bel AJE** (1993) Strategies of phloem loading. *Annu Rev Plant Physiol Plant Mol Biol* **44**: 253–281
- Wallaart RA** (1980) Distribution of sorbitol in Rosaceae. *Phytochemistry* **19**: 2603–2610
- Winter H, Robinson DG, Heldt HW** (1993) Subcellular volumes and metabolite concentrations in barley leaves. *Planta* **191**: 180–190
- Yamaki S** (1980) Properties and functions of sorbitol-6-phosphate dehydrogenase, sorbitol dehydrogenase and sorbitol oxidase in fruit and cotyledon of apple (*Malus pumila* Mill. var. *domestica* Schneid.) *J Jpn Soc Hortic Sci* **49**: 429–434
- Yamaki S** (1987) ATP-promoted sorbitol transport into vacuoles isolated from apple fruit. *Plant Cell Physiol* **28**: 557–564
- Yamaki S, Asakura T** (1988) Energy coupled transport of sorbitol and other sugars into protoplast isolated from apple fruit flesh. *Plant Cell Physiol* **29**: 961–967
- Yamaki S, Ishikawa K** (1986) Roles of four sorbitol related enzymes and invertase in the seasonal alteration of sugar metabolism in apple tissue. *J Am Soc Hortic Sci* **111**: 134–137
- Zimmerman MH, Ziegler H** (1975) List of sugars and sugar alcohols in sieve tube exudates. In M Zimmerman, J Milburn, eds, *Encyclopedia of Plant Physiology, New Series, Vol 1*. Springer-Verlag, Berlin, pp 480–503